Fast measurement of the quadriceps femoris muscle transverse relaxation time at high magnetic field using segmented echo-planar imaging

Alexandre Fouré, Guillaume Duhamel, Christophe Vilmen, David Bendahan, Marc Jubeau, Julien Gondin

Fast Measurement of the Quadriceps Femoris Muscle Transverse Relaxation Time at High Magnetic Field Using Segmented Echo-Planar Imaging

Alexandre Fouré PhD,[1] Guillaume Duhamel PhD,[1] Christophe Vilmen MS,[1] David Bendahan PhD,[1] Marc Jubeau PhD,[1,2] and Julien Gondin PhD[1]*

Purpose: To assess and validate a technique for transverse relaxation time (T_2) measurements of resting and recovering skeletal muscle following exercise with a high temporal resolution and large volume coverage using segmented spin-echo echo-planar imaging (sSE-EPI).
Materials and Methods: Experiments were performed on a 3T magnetic resonance imaging (MRI) scanner using a multislice sSE-EPI technique applied at different echo times (TEs). T_2 measurements were first validated *in vitro* in calibrated T_2 phantoms (range: 25–152 ms) by comparing sSE-EPI, standard spin-echo (SE), and multislice multiecho (MSME) techniques (using a fitting procedure or a 2-TEs calculation). *In vivo* measurements of resting T_2 quadriceps femoris (QF) muscle were performed with both sSE-EPI and MSME sequences. Finally, sSE-EPI was used to quantify T_2 changes in recovering muscle after an exercise.
Results: T_2 values measured *in vitro* with sSE-EPI were similar to those assessed with SE ($P > 0.05$). *In vitro* and *in vivo* T_2 measurements obtained with sSE-EPI were independent of the T_2 determination procedure ($P > 0.05$). In contrast, both *in vitro* and *in vivo* T_2 values derived from MSME were significantly different when using 2-TEs calculation as compared to the fitting procedure ($P < 0.05$). sSE-EPI allowed the detection of increased T_2 values in the QF muscle immediately after exercise ($+14 \pm 9\%$), while lower T_2 values were recorded less than 2 min afterwards ($P < 0.05$).
Conclusion: sSE-EPI sequence is a relevant method to monitor exercise-induced T_2 changes of skeletal muscles over large volume coverage and to detect abnormal patterns of muscle activation.
Level of Evidence: 1

J. MAGN. RESON. IMAGING 2017;45:356–368

The assessment of muscle activity in response to exercise is useful and relevant in sports and rehabilitation medicine. Among other variables, the transverse relaxation time (T_2) measurement has been largely used as a noninvasive index of muscle activation.[1,2] It has been well established that muscle T_2 increases with exercise.[3,4] An exercise-induced T_2 increase has been associated with an increased muscle volume and mainly related to an accumulation of intracellular water.[5,6] During exercise, intracellular water accumulation may result from osmotically[6,7] and/or hydrostatically driven fluid shifts. In addition, a greater level of metabolite accumulation and larger T_2 changes have been reported in predominantly glycolytic as compared to predominantly oxidative muscles.[8] It has also been shown that intracellular acidification could contribute to muscular T_2 changes,[9] demonstrating that muscle metabolic activity could be involved in exercise-induced changes in T_2.[10] Accordingly, intracellular pH-induced T_2 variations are related to changes in magnetization transfer rate between macromolecules and free intracellular water.[9] Considering the rapid recovery rate of intracellular pH at the end of a moderate voluntary exercise,[11] it appears important to

View this article online at wileyonlinelibrary.com. DOI: 10.1002/jmri.25355

Received Mar 17, 2016, Accepted for publication Jun 9, 2016.

The first two authors and the last two authors contributed equally to this work.

*Address reprint requests to: J.G., Centre de Résonance Magnétique Biologique et Médicale (CRMBM), UMR CNRS 7339, Faculté de Médecine la Timone, 27 Boulevard Jean Moulin, 13385 Marseille, France. E-mail: julien.gondin@univ-amu.fr

From the [1]Aix-Marseille Université, CNRS, CRMBM UMR, 7339, Marseille, France; and [2]Université de Nantes, Laboratoire "Motricité, Interactions, Performance," Nantes, France.

obtain fast measurements in order to accurately determine muscle T_2 changes in recovering muscle.[12] This is particularly relevant if we consider that T_2 mapping may provide useful information regarding abnormal patterns of muscle recruitment during exercise[13] and could be used for rehabilitation follow-up of patients/athletes with an impaired muscle function.

Spin-echo-based techniques (such as multislice multiecho technique, MSME), whose signal relation with T_2 exponentially decreases, have been extensively used in numerous skeletal muscle studies.[1,2,14–17] However, it has been largely acknowledged that MSME is very sensitive to instrumental imperfections, resulting in radiofrequency B_1 and static B_0 magnetic field inhomogeneities as well as inefficient crushing schemes.[18,19] Non-ideal 180° refocusing pulses generate T_1-weighted stimulated echoes that inevitably contaminate the T_2 decay curves,[20] thereby leading to a highly unreliable T_2 determination using simple models.[21] Solutions for compensating for the bias introduced by variations in B_1 and B_0 have been proposed but usually require more complex processing or induce other constraints such as acquisition of single slice only.[20,22]

Single spin-echo (SE) techniques can be used for multislice quantitative T_2 measurements by acquiring images at different echo times (TEs). While this approach is less sensitive to B_1 and B_0 errors, it provides a low temporal resolution and is more sensitive to diffusion phenomenon as compared to MSME. The use of echo-planar readout (EPI) can increase the temporal resolution, thereby allowing measurements of dynamic signal changes and/or T_2 values in exercising muscles.[23–26] Given the high sensitivity of EPI to B_0 inhomogeneities, the latter studies were limited to low magnetic field (*i.e.* $B_0 = 1.5$T) and to explorations with a small volume coverage.

Alternatively, non-SE-based techniques can be used to acquire quantitative T_2 images. In particular, variants of steady-state free precession (SSFP) techniques allowed deriving high spatially resolved 3D multiparametric maps (including T_2)[27] within a relatively short acquisition time.[28,29] By sacrificing the spatial resolution and the volume coverage, similar techniques have been used to rapidly assess T_1, T_2, and relative proton density changes in skeletal muscles with a very high temporal resolution (< 150 ms/image).[30]

However, the SSFP-based techniques suffer from several drawbacks including the sensitivity to magnetization transfer effects[31] and the requirement of additional data to avoid artifacts in T_2 maps.[27] More important, these techniques are highly sensitive to B_0 inhomogeneities and T_2 quantification requires accurate determination of the flip angle. At high magnetic field (*i.e.* $B_0 \geq 3$T), this issue is of concern given that B_0 inhomogeneities are larger and dielectric effects can induce nonuniform B_1^+ field[32] resulting in variable flip angle values in different parts of the imaged volume. More advanced refinement of T_2 measurement with SSFP-based techniques has been proposed with the use of partially spoiled SSFP, an approach insensitive to B_0 inhomogeneities, diffusion, and magnetization transfer effects[33] and which can be corrected for nonuniform B_1 issues.[34] However, this approach requires additional scans for correction purposes, thereby greatly increasing the acquisition time.

Overall, the choice of a technique for T_2 measurement would greatly depend on the study requirements. In order to assess T_2 changes in postexercise recovering muscle, a fast and reproducible technique allowing high spatial resolution and large volume coverage, immune to B_0 and B_1 inhomogeneities, and offering a simple T_2 quantification model would be of particular interest. On that basis, we proposed to investigate the use of multislice highly resolved segmented SE-EPI (sSE-EPI) technique acquired at different TEs for T_2 quantification. The number of segments of the sSE-EPI sequence was chosen in order to obtain the best trade-off between image quality and acquisition time.

Materials and methods

Experimental Design

The present work was composed of two investigations (*in vitro* and *in vivo*) including experiments in phantom (Experiment 1) and in healthy subjects (Experiments 2 and 3). Experiments were performed on a whole-body 3T MRI-scanner (VERIO, Siemens Medical System, Erlangen, Germany) using a 6-channel body matrix coil (Siemens). For human investigations, volunteers were fully informed about the nature and the aim of the study and gave their written informed consent to participate. The study was approved by the local Human Research Ethics Committee and was conducted in conformity with the Declaration of Helsinki.

Study 1: In Vitro Experiment

EXPERIMENT 1: IMAGE QUALITY EVALUATION AND T_2 MEASUREMENT VALIDATION IN PHANTOM. EPI is strongly affected by susceptibility-induced artifacts, which are more pronounced with increasing magnetic field. Using a segmenting acquisition scheme, we intended to reduce the EPI readout train and hence the number of phase-encoding steps. The sensitivity of EPI for susceptibility artifacts was then reduced but the acquisition time was increased. Different levels of acquisition segmentation were tested (expressed by the value of echo train length, ETL), *e.g.* for 128 phase-encoding steps required for the image acquisition; ETL = 128 means that a single shot was used (number of segments = 1), whereas ETL = 64 means that 2 segments were used.

Standard spin-echo (SE) sequence, sSE-EPI, and MSME sequences were applied on a T_2-calibrated phantom (TO5-Diagnostic Sonar, Livingston, Scotland) including eight gel tubes with T_2 relaxation times ranging from 50 to 152 ms at 3T (temperature: 294K, accuracy ± 3%) and four additional tubes (T_2: 25, 30, 35, and 40 ms).[35]

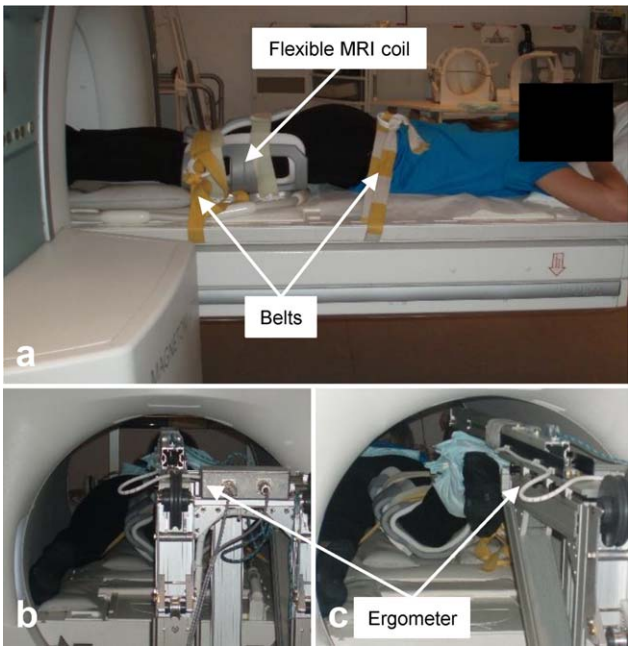

FIGURE 1: Experimental position of the subject inside the 3T MRI scanner with the coil positioned around the right thigh firmly attached to the table with inextensible belts and centered in the magnet (A). During the voluntary exercise, the foot of the subject was attached to a home-made ergometer (B,C).

Common acquisition parameters were: field of view (FOV) = 250 × 250 mm, matrix = 192 × 192, single slice, slice thickness = 10 mm, number of excitations (N_{ex}) = 1, TR = 4250 ms. First- and second-order shimming was performed on the volume of investigation.

Sequence-specific parameters were as follows:

- SE: 8 TE values (20, 30, 40, 50, 60, 70, 80, and 100 ms), bandwidth = 226 Hz/Px. Acquisition time = 8 min 19 s/TE.
- sSE-EPI: 8 TE values (20, 30, 40, 50, 60, 70, 80, and 100 ms), bandwidth = 814 Hz/Px. Four different segmentation schemes were tested, ETL = 9, 13, 25, and 43 leading to acquisition times per TE of 102 s, 60 s, 38 s, and 26 s, respectively. For ETL 43, the first TE was equal to 30 ms. As part of the sSE-EPI sequence provided by the manufacturer, each sSE EPI scan included specific required EPI precalibration adjustments (gradient trajectory measurement, eddy current correction, . . .).
- MSME: 9 TE values (TE = 20, 30, 40, 50, 60, 70, 80, 90, and 100 ms), bandwidth = 226 Hz/Px, total acquisition time = 5 min 03 s.

T_2 maps were generated, from the T_{2w} images obtained at different TEs, by linear fitting on a pixel-by-pixel basis of the signal data logarithm according to Eq. [1] (*i.e.* fitting procedure):

$$Log\Big(S(TE)\Big) = Log(S_0) - (TE/T_2) \qquad (1)$$

where S(TE) is the signal acquired at echo time TE, and S_0 the signal of the equilibrium magnetization. T_2 maps were also generated from a 2-TEs calculation (with TE_1 = 20 ms and TE_2 = 50 ms, *i.e.* $Calc_{20\text{-}50}$, or TE_1 = 30 ms and TE_2 = 60 ms, *i.e.* $Calc_{30\text{-}60}$) using Eq. [2] as extensively used in the literature.[1,2,14]

$$Log\Big(S(TE_1)\Big) - Log\Big(S(TE_2)\Big) = (TE_2 - TE_1)/T_2 \qquad (2)$$

Mean T_2 values were evaluated in regions of interest (ROIs), selected in gel tubes, and manually drawn on T_{2w} image using FSLview (FMRIB, Oxford, UK). Potential distortions of images associated with the ETL factors were visually checked by an experienced researcher (A.F., with 7 years of experience in evaluation of muscle anatomy and geometry).

Study 2: In Vivo Experiments

MRI ACQUISITION. The coil was positioned around the right thigh of the subject placed in prone position (Fig. 1). Imaging parameters for experiments 2 and 3 are summarized in Table 1. The most distal slice was acquired at ~20 mm (*i.e.* ~5% of the thigh length measured for each subject) upper the proximal border of the patella. Similar to *in vitro* experiments, *in vivo* experiments started with first- and second-order shimming procedure and sSE EPI scans included precalibration.

DATA ANALYSIS. Images were analyzed with FSLview and ROIs were manually drawn in each slice looking at the borders of the anatomic cross-sectional area of each muscle of the quadriceps femoris (QF). T_2 maps were generated similar to what was described for Study 1 (*i.e.* fitting procedure and/or 2-TEs calculation). Mean T_2 values for each muscle of the QF (*i.e.* vastus lateralis [VL], vastus medialis [VM], vastus intermedius [VI], and rectus femoris [RF]) was then determined. In the case of potential B_0 inhomogeneities in the most proximal and distal slices generating a visual drop of signal intensity, the corresponding extreme slices were disregarded for analyses. In addition, histograms representing the relative individual muscle volume with respect to T_2 relaxation times were obtained before (PRE) and immediately after the voluntary exercise (POST 0). Relative "activated" volume of each muscle was quantified at POST 0 by considering a threshold for each muscle and each subject, *i.e.* pixels showing a T_2 value > mean + 2 SD of that determined at PRE.

Experiment 2: In Vivo T_2 Measurements of Resting Quadriceps Femoris Muscle

The rationale of this experiment was to compare the resting T_2 values of each skeletal muscle of the QF determined with the sSE-EPI and MSME sequences. T_2 values were determined using both the fitting procedure and the 2-TEs calculation method described in Study 1.

EXPERIMENTAL DESIGN. Thirteen healthy subjects (five females, 30 ± 4 years, 171 ± 8 cm, 65 ± 8 kg) volunteered to participate in this study. For each subject, MRI acquisitions were performed at rest to obtain T_1- and T_2-weighted images (T_{1w} and T_{2w}, respectively). MSME and sSE-EPI sequences were performed in a randomized order.

TABLE 1. MR Sequence Parameters Used for Experiments 2 and 3

	Experiment 2			Experiment 3	
Sequence type	T_{1w}	T_{2w} (MSME)	T_{2w} (sSE-EPI)	T_{1w}	T_{2w} (sSE-EPI)
Repetition time (ms)	490	4250	4250	1320	4250
# Echo time	1	8	5	1	2
Echo time (ms)	13	10/20/30/40/50/60/70/80	20/30/40/50/60	13	20/50
In-plane field of view (mm)	250 × 250	250 × 250	250 × 250	220 × 220	220 × 220
Matrix size	192 × 192	192 × 192	192 × 192	256 × 256	192 × 192
Resolution (mm^2)	1.3 × 1.3	1.6 × 1.3	1.6 × 1.3	0.9 × 0.9	1.4 × 1.1
# slices	15	15	15	22	22
Slice thickness (mm)	10	10	10	8.5	8.5
Gap between slices (mm)	1	1	1	4.25	4.25
Bandwidth (Hz/pixel)	434	226	814	434	814
Fat saturation	No	No	Yes (TI = 230 ms)	No	Yes (TI = 230 ms)
Water excitation	No	No	Yes	No	Yes
Echo train length factor	/	/	13	/	25
# segments	1	1	15	1	8
Phase resolution (%)	100	80	80	100	80
Partial Fourier	No	Yes (6/8)	Yes (6/8)	No	Yes (6/8)
Acquisition time (s)	96	303	300	341	76

MSME: multislice multiecho, sSE-EPI: segmented spin-echo echo-planar imaging, T_1w: T_1-weighted, T_2w: T_2-weighted, TI: inversion time.

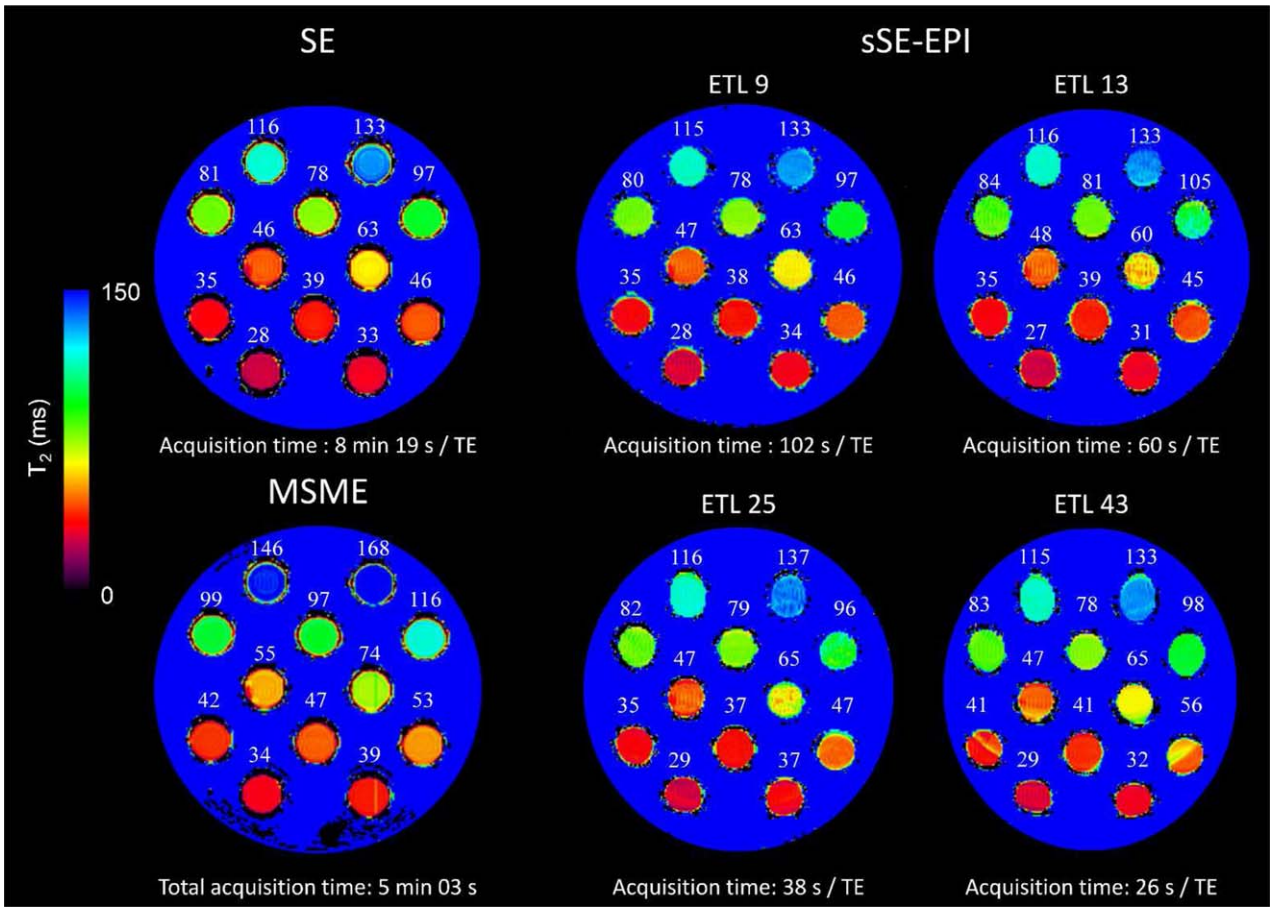

FIGURE 2: T_2 maps of the phantoms and the corresponding mean T_2 values of each gel tube obtained by the fitting procedure on data from the sequences SE, MSME, and sSE-EPI at four ETL factors. Note that the MSME sequence always overestimated the T_2 values as compared to both SE and sSE-EPI sequences.

Experiment 3: In Vivo T_2 Measurements of the Recovering Quadriceps Femoris Muscle After a Submaximal Voluntary Exercise

The objective of this experiment was to assess whether the sSE-EPI sequence can be used to accurately determine the T_2 changes in QF muscle immediately after a submaximal voluntary exercise and the following recovery. Using the large spatial coverage and a high time resolution, we determined the respective T_2 changes in the four individual muscles of the QF and the corresponding kinetics of T_2 recovery.

VOLUNTARY EXERCISE. Subjects were prone within the magnet with the foot attached to a home-made ergometer[36] equipped with a strain gauge (N2A-13-T026P-350; Vishay Micro-Measurements; Vishay Precision Group, Wendell, NC) allowing measuring the force output during exercise. To avoid movement and to limit contraction of other muscles than the QF during the exercise, subjects were firmly attached to the bed of the magnet with three nonelastic straps positioned over the leg, the hip, and the back. The knee of the subject was flexed at ~40° in the resting position. A noncompliant strap was also used to firmly attach the foot of the subjects to the horizontal bars of the ergometer. The force signal was sampled at 1000 Hz using a Powerlab system and Labchart software (ADinstruments, Colorado Springs, CO). Subjects were asked to perform 80 isometric contractions (2 s on, 2 s off) of the knee extensor muscles at 60% (±2.5%) of their maximal voluntary isometric contraction (MVC) force. Real-time visual and auditory feedbacks were provided to the subject to reach and maintain the target force level for 2 s.

EXPERIMENTAL DESIGN. Twelve healthy subjects (two females, 30 ± 4 years, 177 ± 8 cm, 70 ± 10 kg) volunteered to participate in this study. For each subject, MRI investigation was first performed at rest (*i.e.* acquisition of T_{1w} and T_{2w} images, PRE). After a warm-up (*i.e.* 20–25 submaximal voluntary isometric contractions of the knee extensor muscles), MVC force of knee extensors was assessed (*i.e.* three trials of 5 s maximal effort separated by at least 1 min) and a voluntary submaximal exercise was performed in the 3T scanner. Immediately after the exercise, MRI investigation was performed (MR sequence parameters are reported in Table 1) in order to determine the kinetics of T_2 changes with a high time resolution during a 20-min recovery period (*i.e.* from POST 0 to POST 20, 15 T_2 maps were acquired, one T_2 map every 80 s using the sSE-EPI sequence; ETL = 25) and TEs = 20 ms and 50 ms). As part of control for bulk motion, an additional T_{1w} image was acquired at the end of the experiment in order to take into account potential thigh motion within the MRI scanner during the exercise.

TABLE 2. Theoretical T_2 Values of Phantoms and Experimental T_2 Values Assessed with standard Spin-Echo (SE), Segmented SE Echo-Planar Imaging (sSE-EPI) and Multislice Multiecho (MSME) Sequences

	Gel tube		#1	#2	#3	#4	#5	#6
Theoretical T_2			25	30	35	40	50	51
SE		Fit	27.5 ± 1.7	32.5 ± 0.6	35.4 ± 0.8	39.1 ± 0.9	46.0 ± 0.7	46.4 ± 1.8
		$Calc_{20-50}$	27.6 ± 0.7	32.3 ± 0.4	34.9 ± 0.4	39.5 ± 0.7	45.6 ± 0.6	46.5 ± 1.6
		$Calc_{30-60}$	27.5 ± 0.9	32.5 ± 0.5	34.7 ± 0.5	40.1 ± 0.8	45.5 ± 0.8	46.0 ± 2.0
sSE-EPI	ETL 9	Fit	28.3 ± 3.7	33.7 ± 2.5	35.2 ± 2.8	37.9 ± 1.3	46.0 ± 1.2	47.2 ± 2.2
		$Calc_{20-50}$	27.8 ± 1.5	33.1 ± 1.1	35.5 ± 1.3	40.4 ± 0.8	47.2 ± 0.9	47.2 ± 1.8
		$Calc_{30-60}$	27.4 ± 2.0	32.4 ± 1.5	35.6 ± 1.7	39.9 ± 0.9	44.9 ± 1.1	47.7 ± 2.1
	ETL 13	Fit	26.7 ± 2.1	31.3 ± 1.6	34.7 ± 1.8	39.0 ± 0.8	44.6 ± 1.4	48.0 ± 3.3
		$Calc_{20-50}$	27.6 ± 0.9	32.0 ± 0.7	35.3 ± 0.9	39.3 ± 0.5	45.3 ± 1.2	47.3 ± 3.2
		$Calc_{30-60}$	27.3 ± 1.2	31.7 ± 0.8	34.9 ± 1.2	39.0 ± 0.9	44.6 ± 1.7	48.4 ± 3.4
	ETL 25	Fit	28.6 ± 2.5	36.7 ± 2.2	35.3 ± 1.4	37.5 ± 0.7	47.1 ± 1.3	47.0 ± 3.8
		$Calc_{20-50}$	28.3 ± 1.1	33.8 ± 0.9	35.1 ± 0.8	38.8 ± 0.6	45.4 ± 1.4	47.4 ± 2.9
		$Calc_{30-60}$	28.2 ± 1.4	34.3 ± 1.4	35.3 ± 1.0	38.9 ± 0.7	45.4 ± 1.5	48.4 ± 3.6
	ETL 43	Fit	29.2 ± 3.7	32.5 ± 2.5	40.7 ± 8.6	40.8 ± 0.9	56.0 ± 9.1	47.3 ± 3.0
		$Calc_{20-50}$	n/a	n/a	n/a	n/a	n/a	n/a
		$Calc_{30-60}$[a]	28.3 ± 1.5	32.2 ± 1.3	35.1 ± 4.3	40.4 ± 0.7	51.3 ± 5.3	46.8 ± 2.3
MSME		Fit	33.5 ± 1.0	39.1 ± 0.4	41.8 ± 0.5	46.7 ± 0.9	53.1 ± 0.7	55.3 ± 1.6
		$Calc_{20-50}$[a][b]	28.8 ± 0.7	33.5 ± 0.3	36.1 ± 0.5	40.6 ± 0.8	46.3 ± 0.6	47.4 ± 1.4
		$Calc_{30-60}$[b]	35.0 ± 1.1	40.4 ± 0.7	43.1 ± 0.9	47.1 ± 1.0	52.6 ± 0.8	55.5 ± 1.8

T_2 values are expressed in ms (mean ± SD). Only phantoms with T_2 values in the range of physiological values for skeletal muscle were reported. Accuracy of theoretical T_2 values of phantoms was ± 3%. ETL: echo train length factor, Fit: T_2 values assessed from T_2 maps determined with the fitting procedure on 5 TEs for sSE-Epi and 8 TEs for MSME, $Calc_{20-50}$: T_2 values assessed from T_2 maps determined with the 2-TEs calculation using images at TE 20 ms and 50 ms, $Calc_{30-60}$: T_2 values assessed from T_2 maps determined with the 2-TEs calculation using images at TE 30 ms and 60 ms.

[a]Significantly different than T_2 values determined with the fitting procedure.

[b]Significantly different than T_2 values determined with $Calc_{20-50}$.

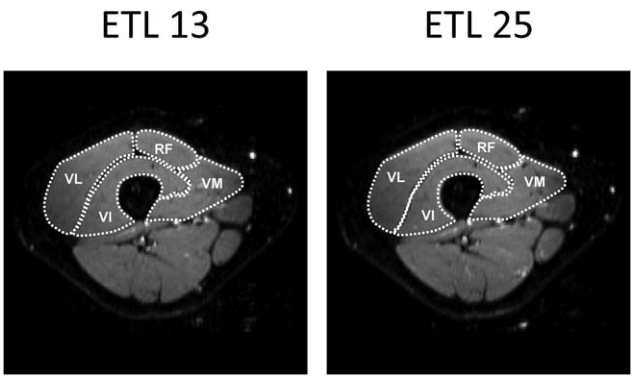

FIGURE 3: Typical resting T_2-weighted images of the thigh muscles obtained with segmented SE EPI sequence for two ETL. The four muscles of the quadriceps femoris were delineated with dotted lines (VL: vastus lateralis, RF: rectus femoris, VM: vastus medialis, VI: vastus intermedius).

A reproducibility experiment was performed in six subjects (three females, 30 ± 4 years, 171 ± 9 cm, 64 ± 7 kg) who took part in two MRI experimental sessions separated by at least 7 days in order to determine the standard error (SEM) of T_2 measurements and the corresponding coefficient of variation (CV) in the four muscles of the QF.

Statistics

After checking the distribution of data using the Shapiro–Wilk test, parametric statistical tests were performed using Statistica software (Statsoft, Tulsa, OK). One-way analysis of variance (ANOVA) was performed to compare T_2 values in phantom among MR sequences (SE, sSE-EPI, and MSME). Two-way ANOVA (MR sequence * muscle) was used to identify potential differences in T_2 values at rest in the four muscles of the QF using sSE-EPI and MSME sequences. Two-way repeated-measures ANOVA (muscle * time) was used to determine potential differences in T_2 changes after exercise in the four muscles of the QF. A Tukey's HSD post-hoc analysis was performed when appropriate. The level of significance was set at $P < 0.05$. Results are reported as mean ± SD.

RESULTS

Study 1: In Vitro Experiments

EXPERIMENT 1: IMAGE QUALITY EVALUATION AND T_2 MEASUREMENT VALIDATION IN PHANTOM. Figure 2 shows the T_2 maps of the phantom obtained by the linear fitting procedure for MSME, SE, and sSE-EPI (ETL 9, ETL13, ETL25, and ETL43) data. T_2 values obtained with SE and sSE-EPI sequences were not statistically different ($P > 0.87$), whereas those obtained with MSME were always significantly higher than those of both SE and sSE-EPI sequences ($P < 0.05$). Negligible distortions were observed in images obtained with sSE-EPI sequences using ETL factors of 9 and 13, whereas moderate and strong distortions were observed for ETL 25 and ETL 43, respectively (Fig. 2). A large within-ROI variability of T_2 measurements was quantified for sSE-EPI ETL 43 (Table 2) and the corresponding T_2 values determined with the fitting procedure were significantly higher than those assessed with 2-TEs calculation ($P < 0.05$). For the MSME sequence, T_2 values determined with 2-TEs calculation using TEs of 20 ms and 50 ms were significantly lower than those obtained with either the fitting procedure or the 2-TEs calculation using TEs of 30 ms and 60 ms ($P < 0.05$, Table 2).

Overall, phantom experiments clearly showed that both sSE-EPI sequences with ETL factors of 13 and 25 allowed getting T_2 maps with high temporal (acquisition time $\leq$60 s/TE) and spatial resolution while suffering from only negligible distortions (Fig. 2), that ultimately result in similar T_2 values ($P = 0.99$, Table 2). These configurations were chosen for *in vivo* experiments, whereas sSE-EPI sequences with ETL 9 and 43 were disregarded due to too long acquisition time (for ETL 9, 102 s/TE) and both marked distortions and high within-ROI variability for the T_2 values (ETL 43). It is noteworthy that distortions appeared larger on phantom images as compared to *in vivo* acquisitions (Fig. 3).

Study 2: In Vivo Experiments

EXPERIMENT 2: IN VIVO T_2 MEASUREMENTS OF RESTING QUADRICEPS FEMORIS MUSCLE. In line with the findings of Experiment 1, quantitative analyses performed in the QF muscle showed that T_2 values determined from MSME sequence were significantly higher ($P < 0.05$) as compared to those obtained from sSE-EPI sequences (Table 3). The TE values strongly influenced T_2 values derived from the MSME sequence (Fig. 4) as illustrated by the lower and higher T_2 values obtained with $Calc_{20\text{-}50}$ and $Calc_{30\text{-}60}$ as compared to T_2 maps generated with eight TEs, respectively (Table 3). On the contrary, sSE-EPI was very robust to TE values and averaged T_2 values assessed in the four muscles of the QF were independent of the method used to determine the T_2 map (*i.e.* fitting procedure or 2-TEs calculation) (Table 3).

EXPERIMENT 3: IN VIVO T_2 MEASUREMENTS OF THE RECOVERING QUADRICEPS FEMORIS MUSCLE AFTER A SUBMAXIMAL VOLUNTARY EXERCISE. Reproducibility of T_2 measurements in resting muscles with sSE-EPI (*i.e.* $Calc_{20\text{-}50}$) was very good, as illustrated by the SEM lower than 0.8 ms (RF: 0.6 ms, VI: 0.6 ms, VL: 0.7 ms, VM: 0.8 ms, QF: 0.6 ms) and the CV lower than 2.5% (RF: 1.9%, VI: 2.1%, VL: 2.3%, VM: 2.5%, QF: 2.2%). Resting T_2 values obtained before the voluntary exercise for each muscle of the QF (29.6 ± 0.8 ms) were similar to those obtained in Experiment 2 (29.1 ± 0.7 ms). The exercise led to a significant T_2 increase in the four muscles of the QF ($P < 0.05$, Table 4). The T_2 increase immediately after the voluntary exercise (*i.e.* POST 0) was significantly higher in the RF as compared to both VL and VM muscles ($P < 0.05$, Table 4). As shown in Figure 5, a rightward shift in the

TABLE 3. Resting T_2 Values Using Segmented Spin-Echo Echo-Planar Imaging (sSE-EPI) and Multislice Multiecho (MSME) Sequences on the Quadriceps Femoris Muscle ($N = 13$)

		VL	RF	VM	VI	QF
sSE-EPI	Fit	29.6 ± 0.7 [29.2 – 30.0]	29.3 ± 0.7 [28.9 – 29.7]	29.6 ± 1.1 [29.0 – 30.1]	29.4 ± 0.9 [28.9 – 29.9]	29.5 ± 0.7 [29.1 – 29.9]
	$Calc_{20-50}$	29.2 ± 0.8 [28.7 – 29.6]	28.9 ± 0.8 [28.4 – 29.3]	29.3 ± 1.0 [28.7 – 29.8]	29.0 ± 1.0 [28.4 – 29.5]	29.1 ± 0.7 [28.7 – 29.5]
	$Calc_{30-60}$	30.4 ± 0.7 [30.0 – 30.8]	30.1 ± 0.7 [29.7 – 30.5]	30.3 ± 1.2 [29.6 – 30.9]	30.1 ± 1.0 [29.5 – 30.7]	30.2 ± 0.8 [29.8 – 30.6]
MSME	Fit	29.8 ± 1.7 [28.9 – 30.7]	30.8 ± 1.5[b] [30.0 – 31.6]	30.8 ± 1.3 [30.1 – 31.5]	31.5 ± 2.8[a,c] [30.0 – 33.0]	30.8 ± 1.4[a,b] [30.0 – 31.5]
	$Calc_{20-50}$	27.6 ± 0.8[a,d] [27.1 – 28.0]	27.9 ± 0.9[c,d] [27.4 – 28.3]	27.9 ± 1.6[a,d] [27.1 – 28.8]	28.1 ± 0.6[c,d] [27.7 – 28.4]	27.9 ± 0.8[a,d] [27.5 – 28.3]
	$Calc_{30-60}$	34.9 ± 1.2[a,e] [34.2 – 35.6]	36.4 ± 2.0[a,e] [35.3 – 37.5]	36.9 ± 3.0[a,e] [35.2 – 38.5]	38.0 ± 1.7[a,e] [37.1 – 38.9]	36.6 ± 1.2[a,e] [35.9 – 37.2]

T_2 values are expressed in ms (mean ± SD [95% confidence interval]). Fit: T_2 values assessed from T_2 maps determined with the fitting procedure on 5 TEs for sSE-EPI and 8 TEs for MSME, $Calc_{20-50}$: T_2 values assessed from T_2 maps determined with the 2-TEs calculation using images at TE 20 ms and 50 ms, $Calc_{30-60}$: T_2 values assessed from T_2 maps determined with the 2-TEs calculation using images at TE 30 ms and 60 ms, VL: vastus lateralis, RF: rectus femoris, VM: vastus medialis, VI: vastus intermedius, QF: quadriceps femoris.
[a]Different from sSE-EPI fit.
[b]Different from sSE-EPI $Calc_{20-50}$.
[c]Different from sSE-EPI $Calc_{30-60}$.
[d]Different from MSME fit.
[e]Different from MSME $Calc_{20-50}$.

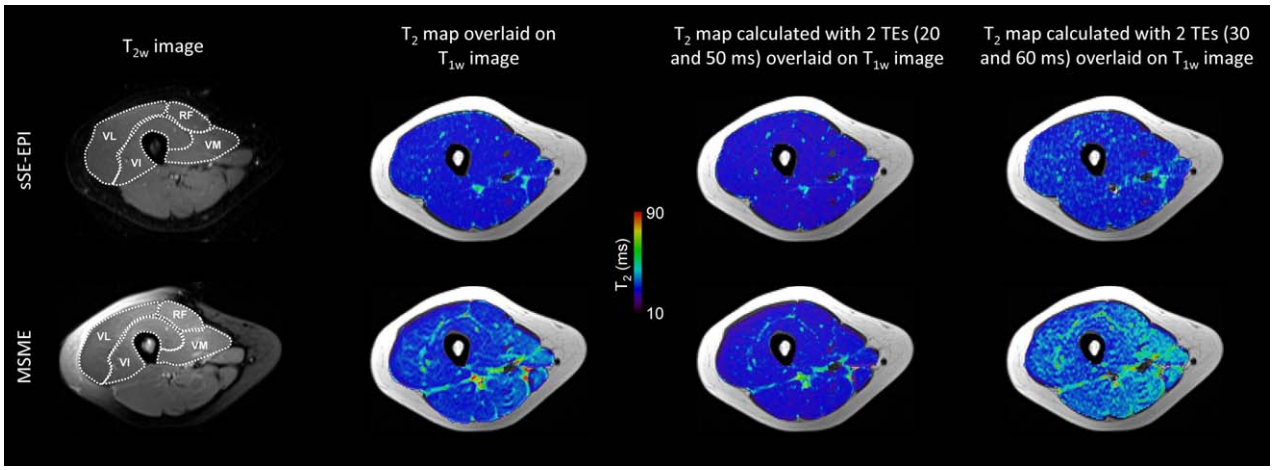

FIGURE 4: Typical resting T_2-weighted images and T_2 maps (overlaid on T_1-weighted images) of the thigh muscles obtained with MSME and sSE-EPI. The four muscles of the quadriceps femoris were delineated with dotted lines (VL: vastus lateralis, RF: rectus femoris, VM: vastus medialis, VI: vastus intermedius).

relationships between the relative muscle volume and the voxel-T_2 value was observed in the four muscles but appeared larger for the RF, despite a large variability among individuals (relative "activated" muscle volume: RF = 52 ± 26%, VI = 29 ± 29%, VL = 26 ± 34%, VM = 33 ± 36%). Peak T_2 occurred immediately after exercise (QF: + 14 ± 9%, VL: + 10 ± 11%, RF: + 21 ± 8%, VM: + 11 ± 11%, VI: + 15 ± 10%, *i.e.* relative T_2 changes at POST 0 as compared to PRE) while T_2 values decreased during the 20-min recovery period (QF: –8 ± 5%, VL: –6 ± 6%, RF: –11 ± 4%, VM: –7 ± 7%, VI: –8 ± 5%, *i.e.* relative T_2 changes at POST 20 as compared to POST 0). It is noteworthy that significantly lower T_2 values were found less than 2 min after the end of the exercise as compared to the T_2 peak values (*i.e.*, at POST 0) (Fig. 6).

Discussion

In the present study, we demonstrated that sSE-EPI, a widespread technique, can be used to simply measure T_2 values of QF muscles at high magnetic field (3T). Using the sSE-EPI sequence, the degree of EPI segmentation can be chosen in order to achieve the best compromise between image quality and acquisition time. On that basis, T_2 maps rapidly determined over a large spatial coverage were sufficiently sensitive to assess changes in skeletal muscle T_2 values after a submaximal voluntary exercise and accurately follow its recovery.

In order to address the issues related to dynamic T_2 measurements in skeletal muscle after a standardized exercise (*e.g.* sensitivity to B_1 and B_0 inhomogeneities, low spatial coverage), we investigated the performance of a segmented SE-EPI approach at high magnetic field (3T). The number of EPI segments was adjusted in order to achieve the best trade-off between image distortion and acquisition time. On

TABLE 4. T_2 Values Determined at Rest (PRE), at the End of a Submaximal Voluntary Exercise (POST 0) and After 20 Min of Recovery (POST 20) in the Four Muscles of the Quadriceps Femoris ($N = 12$)

	PRE	POST 0	POST 20
VL	29.8 ± 0.8 [29.3 – 30.2]	33.1 ± 3.2[a] [31.3 – 34.9]	30.6 ± 1.1[b] [30.0 – 31.3]
RF	29.7 ± 1.1 [29.1 – 30.3]	35.7 ± 2.8[a,c,d] [34.1 – 37.3]	31.9 ± 1.8[b] [30.9 – 32.9]
VM	29.5 ± 0.7 [29.1 – 29.8]	33.2 ± 3.3[a] [31.3 – 35.0]	30.3 ± 1.0[b] [29.7 – 30.8]
VI	29.7 ± 0.8 [29.3 – 30.2]	34.5 ± 3.1[a] [32.7 – 36.2]	31.4 ± 1.3[b] [30.6 – 32.1]
QF	29.6 ± 0.8 [29.2 – 30.1]	34.1 ± 2.9[a] [32.4 – 35.7]	31.0 ± 1.2[b] [30.4 – 31.7]

T_2 values are expressed in ms (mean ± SD [95% confidence interval]). VL: vastus lateralis, RF: rectus femoris, VM: vastus medialis, VI: vastus intermedius, QF: quadriceps femoris.
[a]Different from PRE.
[b]Different from POST 0.
[c]Different from VM.
[d]Different from VL.

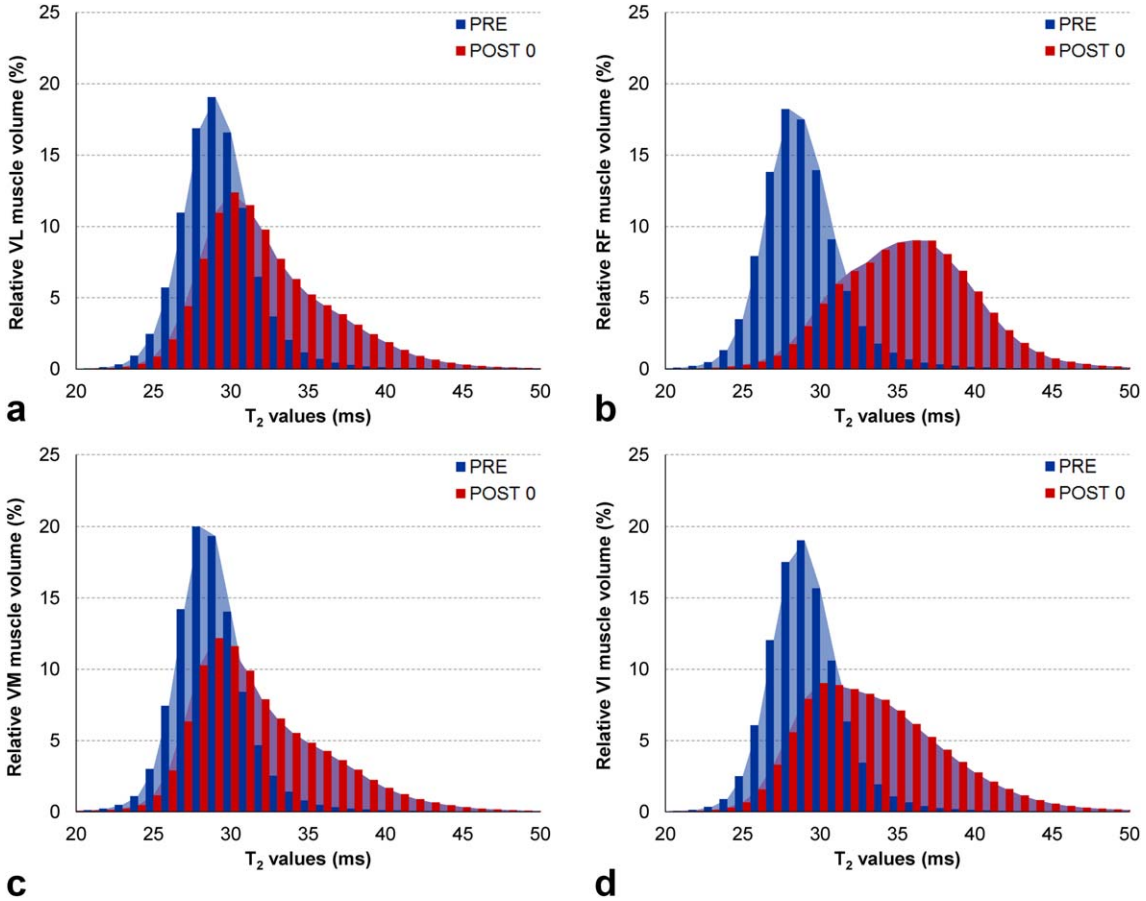

FIGURE 5: Distribution of T_2 values with respect to the relative volume of each muscle (A: vastus lateralis [VL], B: rectus femoris [RF], C: vastus medialis [VM] and D: vastus intermedius [VI]) before and after the voluntary exercise. Distribution of T_2 values is roughly similar among muscles before the exercise. In contrast, a larger rightward shift is observed after the exercise for the RF (and in less proportion in the VI) as compared to the VL and the VM muscles.

that basis, an ETL factor ranging between 13 and 25 minimized distortions, while offering image acquisition times ranging between 38 and 60 s/TE with a high spatial resolution (i.e. 1.3–1.7 mm^2 in plane resolution) and a large spatial coverage (22 slices).

Quantitative T_2 measurements obtained with sSE-EPI were first validated *in vitro* on phantoms with T_2 values included in the physiological range of those observed in skeletal muscle.[2,14,15,37] T_2 values determined with sSE-EPI were similar to those assessed with the SE sequence. As expected, higher T_2 values were systematically found with MSME for all configurations (*i.e.* fitting procedure, 2-TEs calculation, *in vitro*, and *in vivo* experiments). In addition, T_2 values determined with a 2-TEs calculation for MSME were highly dependent on the selected TE values. The latter result is mainly due to the generation of stimulated echoes that contaminate the T_2 decay curves.[20,21] The fitting and 2-TEs calculation approaches gave similar results for sSE-EPI, further highlighting stronger robustness of sSE-EPI as compared to MSME to rapidly determine T_2 changes in skeletal muscle over a large spatial coverage with the 2-TEs calculation method.

The sensitivity of sSE-EPI to detect rapid and subtle T_2 changes was further illustrated by the lower T_2 values recorded less than 2 min after the end of exercise as compared to the T_2 peak values (*i.e.* at POST 0). This rapid T_2 recovery may be related to changes in intracellular water accumulation volume and acidosis, as previously suggested.[6,9] Exercise-induced T_2 changes have been assessed in a large number of studies using long total acquisition time (4–5 min).[1,2,38–40] Therefore, the T_2 measurements over such a long period of time inevitably represent an averaged value which does underestimate the extent of T_2 changes. In addition, the estimation of the relative muscle contribution involved in a motor task can be biased if the kinetics of T_2 differ among muscle, as recently shown for the triceps surae muscle.[12] In the latter study, Varghese *et al.* reduced the MRI acquisition time using an SSFP sequence.[12] Although exercise-induced relative T_2 increase in triceps surae muscle was in the same range (~10%) to what has been determined for QF muscle in the present study, it should be pointed out that the spatial coverage was limited to the acquisition of a single axial slice.[12] Considering that potential heterogeneity in muscle activation can occur along the

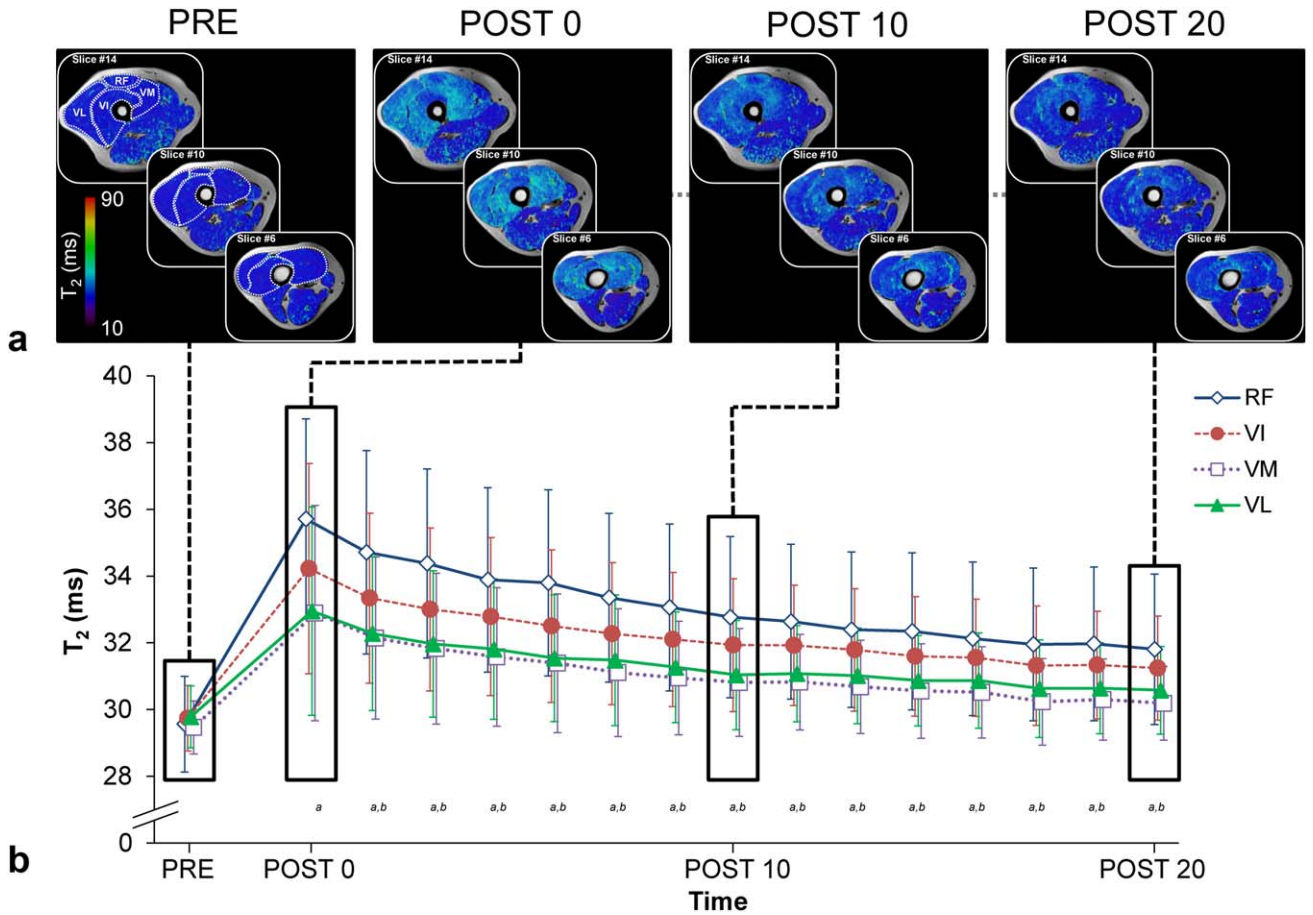

FIGURE 6: A: T_2 maps (overlaid on T_1-weighted image) of thigh muscles obtained with sSE-EPI for one subject before (PRE), immediately after a voluntary isometric exercise (POST 0) and during recovery (10 min [POST 10] and 20 min [POST 20] after the end of the exercise). The four muscles of the quadriceps femoris are delineated with dotted lines at baseline (VL: vastus lateralis, RF: rectus femoris, VM: vastus medialis, VI: vastus intermedius). T_2 was homogenously increased along each muscle of the quadriceps femoris after the voluntary exercise with a peak at POST 0. B: Kinetics of T_2 values during recovery in each muscle of QF (vastus lateralis [VL], vastus medialis [VM], rectus femoris [RF] and vastus intermedius [VI], $N = 12$). Time effect: [a]different from PRE, [b]different from POST 0.

muscle length,[14] among muscles within a muscle group,[41] between individuals,[42] and according to the contraction modality (*e.g.* voluntary *vs.* electrically evoked contractions),[43] it is essential to explore a large muscle volume to be representative of the whole muscle activity. Hence, the sSE-EPI sequence appears as a relevant strategy for assessing muscle activation with a combination of high spatial and temporal resolutions over a large spatial coverage and a low sensitivity to B_1 and B_0 inhomogeneities. Interestingly, we found heterogeneous activation patterns among the four muscles of the QF in response to the exercise. Indeed, T_2 changes were significantly higher in the RF as compared to both VL and VM muscles, which is in accordance with our previous study performed at a lower force level.[44] It is noteworthy that a high interindividual variability was also observed in the T_2 changes induced by the exercise. It is well established that the profile (endurance/explosive) and/or the training status of the volunteers (from recreationally active volunteers performing an unaccustomed exercise to volunteers trained in endurance exercises) can contribute to the interindividual difference in relative contribution of the QF muscle during an exercise performed at 60% MVC.[45] In that way, the combination of sSE-EPI sequence with a newly developed methodology based on statistical parametric mapping[46] would allow accurately localizing muscle activation according to the muscle contraction modality (*e.g.* voluntary *vs.* electrically evoked[44] or concentric *vs.* eccentric[47]).

One of the limitations of the current study could be related to a slightly short second TE used in Experiment 3 (i.e., 50 ms). We considered that the longest TE should have been theoretically 20–60% higher than the highest measured T_2 values (*i.e.* from 31 ms to 42 ms) in order to obtain an accurate T_2 measurement. However, we observed no difference whether T_2 was calculated using 2-TEs (*i.e.* 20–50 ms and 30–60 ms) or using a linear fit (with T_2 values ranging from 25–51 ms). On that basis, one could assume that the influence of the selected maximal TE value

on T_2 measurements in our study is negligible. Considering that the T_2 calculation with 2-TEs is independent of the TE values for sSE-EPI, the choice of TEs could be modulated according to the experimental context, *i.e.* if the T_2 increase is expected to be higher than 40–45 ms, longer TEs should be used. Another potential limitation could be related to the influence of muscle fatty infiltration on T_2 measurements, considering the higher T_2 value of the fat tissue as compared to skeletal muscle.[48] However, we included in the present study young (age ranged from 25–37 years old), healthy, and relatively active subjects for whom intramuscular fatty infiltration was negligible. Furthermore, we used a fat saturation scheme with the sSE EPI sequence in order to further limit the influence of fat on T_2 values. As a result, one could rule out any effect of fatty infiltration on our T_2 measurements. However, full suppression of the fat signal is extremely challenging when performing MRI investigations over a large volume coverage in fat-infiltrated tissues. Therefore, further studies are needed to determine if the sSE-EPI sequence with fat saturation is appropriate for evaluating muscle water T_2 in patients with large fatty infiltrations. It should be kept in mind that our proof-of-concept study clearly highlights both the sensitivity and accuracy of sSE-EPI sequence for monitoring rapid T_2 changes in healthy skeletal muscle. This method is relevant for assessing changes in muscle activation patterns in athletes/subjects with impaired muscle function.[13]

In conclusion, we demonstrated that the sSE-EPI sequence is a valid and fast method for assessing changes in T_2 skeletal muscle with a large spatial coverage at high magnetic field. Considering the straight and simple postprocessing and the sequence availability in clinical scanners, this method would offer new opportunities for evaluating skeletal muscle activation pattern in response to exercise.

Acknowledgments

Contract grant sponsor: Centre National de la Recherche Scientifique; contract grant number: CNRS UMR 7339.
The authors thank Dr. Sylviane Confort-Gouny, Dr. Michaël Sdika, Dr. Alexandre Vignaud, and Patrick Viout for help in data acquisition and processing, the Assistance Publique des Hôpitaux de Marseille (APHM), and all the subjects who participated in the study.

References

1. Adams GR, Harris RT, Woodard D, Dudley GA. Mapping of electrical muscle stimulation using MRI. J Appl Physiol 1993;74:532–537.
2. Kinugasa R, Kawakami Y, Fukunaga T. Mapping activation levels of skeletal muscle in healthy volunteers: an MRI study. J Magn Reson Imaging 2006;24:1420–1425.
3. Bratton CB, Hopkins AL, Weinberg JW. Nuclear magnetic resonance studies of living muscle. Science 1965;147:738–739.
4. Fleckenstein JL, Canby RC, Parkey RW, Peshock RM. Acute effects of exercise on MR imaging of skeletal muscle in normal volunteers. AJR Am J Roentgenol 1988;151:231–237.
5. Reid RW, Foley JM, Jayaraman RC, Prior BM, Meyer RA. Effect of aerobic capacity on the T(2) increase in exercised skeletal muscle. J Appl Physiol (1985) 2001;90:897–902.
6. Damon BM, Gregory CD, Hall KL, Stark HJ, Gulani V, Dawson MJ. Intracellular acidification and volume increases explain R(2) decreases in exercising muscle. Magn Reson Med 2002;47:14–23.
7. Meyer RA, Prior BM, Siles RI, Wiseman RW. Contraction increases the T(2) of muscle in fresh water but not in marine invertebrates. NMR Biomed 2001;14:199–203.
8. Prior BM, Ploutz-Snyder LL, Cooper TG, Meyer RA. Fiber type and metabolic dependence of T2 increases in stimulated rat muscles. J Appl Physiol 2001;90:615–623.
9. Louie EA, Gochberg DF, Does MD, Damon BM. Transverse relaxation and magnetization transfer in skeletal muscle: effect of pH. Magn Reson Med 2009;61:560–569.
10. Patten C, Meyer RA, Fleckenstein JL. T2 mapping of muscle. Semin Musculoskelet Radiol 2003;7:297–305.
11. Fouré A, Wegrzyk J, Le Fur Y, et al. Impaired mitochondrial function and reduced energy cost as a result of muscle damage. Med Sci Sports Exerc 2015;47:1135–1144.
12. Varghese J, Scandling D, Joshi R, et al. Rapid assessment of quantitative T1, T2 and T2* in lower extremity muscles in response to maximal treadmill exercise. NMR Biomed 2015;28:998–1008.
13. Pattyn E, Verdonk P, Steyaert A, Van Tiggelen D, Witvrouw E. Muscle functional MRI to evaluate quadriceps dysfunction in patellofemoral pain. Med Sci Sports Exerc 2013;45:1023–1029.
14. Black CD, Elder CP, Gorgey A, Dudley GA. High specific torque is related to lengthening contraction-induced skeletal muscle injury. J Appl Physiol 2008;104:639–647.
15. Prior BM, Foley JM, Jayaraman RC, Meyer RA. Pixel T2 distribution in functional magnetic resonance images of muscle. J Appl Physiol (1985) 1999;87:2107–2114.
16. Prior BM, Jayaraman RC, Reid RW, et al. Biarticular and monoarticular muscle activation and injury in human quadriceps muscle. Eur J Appl Physiol 2001;85:185–190.
17. Guilhem G, Hug F, Couturier A, et al. Effects of air-pulsed cryotherapy on neuromuscular recovery subsequent to exercise-induced muscle damage. Am J Sports Med 2013;41:1942–1951.
18. Majumdar S, Orphanoudakis SC, Gmitro A, O'Donnell M, Gore JC. Errors in the measurements of T2 using multiple-echo MRI techniques. I. Effects of radiofrequency pulse imperfections. Magn Reson Med 1986;3:397–417.
19. Majumdar S, Orphanoudakis SC, Gmitro A, O'Donnell M, Gore JC. Errors in the measurements of T2 using multiple-echo MRI techniques. II. Effects of static field inhomogeneity. Magn Reson Med 1986;3:562–574.
20. Lebel RM, Wilman AH. Transverse relaxometry with stimulated echo compensation. Magn Reson Med 2010;64:1005–1014.
21. Marty B, Baudin PY, Reyngoudt H, et al. Simultaneous muscle water T and fat fraction mapping using transverse relaxometry with stimulated echo compensation. NMR Biomed 2016;29:431–443.
22. Sled JG, Pike GB. Correction for B(1) and B(0) variations in quantitative T(2) measurements using MRI. Magn Reson Med 2000;43:589–593.
23. Disler DG, Cohen MS, Krebs DE, Roy SH, Rosenthal DI. Dynamic evaluation of exercising leg muscle in healthy subjects with echo planar MR imaging: work rate and total work determine rate of T2 change. J Magn Reson Imaging 1995;5:588–593.

24. Kennan RP, Price TB, Gore JC. Dynamic echo planar imaging of exercised muscle. Magn Reson Imaging 1995;13:935–941.

25. Ploutz-Snyder LL, Nyren S, Cooper TG, Potchen EJ, Meyer RA. Different effects of exercise and edema on T2 relaxation in skeletal muscle. Magn Reson Med 1997;37:676–682.

26. Tawara N, Nitta O, Kuruma H, Niitsu M, Itoh A. T2 mapping of muscle activity using ultrafast imaging. Magn Reson Med Sci 2011;10: 85–91.

27. Deoni SC. Transverse relaxation time (T2) mapping in the brain with off-resonance correction using phase-cycled steady-state free precession imaging. J Magn Reson Imaging 2009;30:411–417.

28. Schmitt P, Griswold MA, Jakob PM, et al. Inversion recovery TrueFISP: quantification of T(1), T(2), and spin density. Magn Reson Med 2004; 51:661–667.

29. Newbould RD, Skare ST, Alley MT, Gold GE, Bammer R. Three-dimensional T(1), T(2) and proton density mapping with inversion recovery balanced SSFP. Magn Reson Imaging 2010;28:1374–1382.

30. de Sousa PL, Vignaud A, Fleury S, Carlier PG. Fast monitoring of T(1), T(2), and relative proton density (M(0)) changes in skeletal muscles using an IR-TrueFISP sequence. J Magn Reson Imaging 2011;33:921–930.

31. Crooijmans HJ, Gloor M, Bieri O, Scheffler K. Influence of MT effects on T(2) quantification with 3D balanced steady-state free precession imaging. Magn Reson Med 2011;65:195–201.

32. Schick F. Whole-body MRI at high field: technical limits and clinical potential. Eur Radiol 2005;15:946–959.

33. Bieri O, Scheffler K, Welsch GH, Trattnig S, Mamisch TC, Ganter C. Quantitative mapping of T2 using partial spoiling. Magn Reson Med 2011;66:410–418.

34. de Sousa PL, Vignaud A, Caldas de Almeida Araujo E, Carlier PG. Factors controlling T2 mapping from partially spoiled SSFP sequence: optimization for skeletal muscle characterization. Magn Reson Med 2012;67:1379–1390.

35. Wang G, El-Sharkawy AM, Edelstein WA, Schar M, Bottomley PA. Measuring T(2) and T(1), and imaging T(2) without spin echoes. J Magn Reson 2012;214:273–280.

36. Layec G, Bringard A, Le Fur Y, et al. Reproducibility assessment of metabolic variables characterizing muscle energetics in vivo: A 31P-MRS study. Magn Reson Med 2009;62:840–854.

37. Arpan I, Forbes SC, Lott DJ, et al. T(2) mapping provides multiple approaches for the characterization of muscle involvement in neuromuscular diseases: a cross-sectional study of lower leg muscles in 5-15-year-old boys with Duchenne muscular dystrophy. NMR Biomed 2013;26:320–328.

38. Kinugasa R, Kawakami Y, Fukunaga T. Muscle activation and its distribution within human triceps surae muscles. J Appl Physiol 2005;99: 1149–1156.

39. Adams GR, Duvoisin MR, Dudley GA. Magnetic resonance imaging and electromyography as indexes of muscle function. J Appl Physiol (1985) 1992;73:1578–1583.

40. Cheng HA, Robergs RA, Letellier JP, Caprihan A, Icenogle MV, Haseler LJ. Changes in muscle proton transverse relaxation times and acidosis during exercise and recovery. J Appl Physiol (1985) 1995;79: 1370–1378.

41. Wakahara T, Ema R, Miyamoto N, Kawakami Y. Inter- and intramuscular differences in training-induced hypertrophy of the quadriceps femoris: association with muscle activation during the first training session. Clin Physiol Funct Imaging 2015 [Epub ahead of print].

42. Hug F, Bendahan D, Le Fur Y, Cozzone PJ, Grelot L. Heterogeneity of muscle recruitment pattern during pedaling in professional road cyclists: a magnetic resonance imaging and electromyography study. Eur J Appl Physiol 2004;92:334–342.

43. Ogino M, Shiba N, Maeda T, et al. MRI quantification of muscle activity after volitional exercise and neuromuscular electrical stimulation. Am J Phys Med Rehabil 2002;81:446–451.

44. Jubeau M, Le Fur Y, Duhamel G, et al. Localized metabolic and t2 changes induced by voluntary and evoked contractions. Med Sci Sports Exerc 2015;47:921–930.

45. Layec G, Bringard A, Le Fur Y, et al. Comparative determination of energy production rates and mitochondrial function using different 31P MRS quantitative methods in sedentary and trained subjects. NMR Biomed 2011;24:425–438.

46. Fouré A, Le Troter A, Guye M, Mattei JP, Bendahan D, Gondin J. Localization and quantification of intramuscular damage using statistical parametric mapping and skeletal muscle parcellation. Sci Rep 2015;5:18580.

47. Ono T, Okuwaki T, Fukubayashi T. Differences in activation patterns of knee flexor muscles during concentric and eccentric exercises. Res Sports Med 2010;18:188–198.

48. Gold GE, Han E, Stainsby J, Wright G, Brittain J, Beaulieu C. Musculoskeletal MRI at 3.0 T: relaxation times and image contrast. AJR Am J Roentgenol 2004;183:343–351.